Molecular Cell 22, 741–753, June 23, 2006 ©2006 Elsevier Inc. DOI 10.1016/j.molcel.2006.05.015

Structural Basis of DNA Recognition by p53 Tetramers

Malka Kitayner,[1] Haim Rozenberg,[1] Naama Kessler,[1] Dov Rabinovich,[1] Lihi Shaulov,[2] Tali E. Haran,[2,*] and Zippora Shakked[1,*]
[1] Department of Structural Biology
Weizmann Institute of Science
Rehovot 76100
[2] Department of Biology
Technion
Technion City
Haifa 32000
Israel

Summary

The tumor-suppressor protein p53 is among the most effective of the cell's natural defenses against cancer. In response to cellular stress, p53 binds as a tetramer to diverse DNA targets containing two decameric half-sites, thereby activating the expression of genes involved in cell-cycle arrest or apoptosis. Here we present high-resolution crystal structures of sequence-specific complexes between the core domain of human p53 and different DNA half-sites. In all structures, four p53 molecules self-assemble on two DNA half-sites to form a tetramer that is a dimer of dimers, stabilized by protein-protein and base-stacking interactions. The protein-DNA interface varies as a function of the specific base sequence in correlation with the measured binding affinities of the complexes. The new data establish a structural framework for understanding the mechanisms of specificity, affinity, and cooperativity of DNA binding by p53 and suggest a model for its regulation by regions outside the sequence-specific DNA binding domain.

Introduction

The loss of p53 activity is a critical event in cancer development. A major mechanism by which p53 acts as a tumor suppressor is as a transcription factor, regulating the expression of a range of downstream genes in response to cellular stresses (Oren, 2003; Prives and Hall, 1999; Vogelstein et al., 2000; Vousden and Lu, 2002). The activity of p53 is modulated by posttranslational modifications such as phosphorylation and acetylation as well as by other proteins (Jayaraman and Prives, 1999). The activation of p53-dependent genes can initiate a cascade of signal transduction pathways leading to different cellular responses including cell-cycle arrest and apoptosis, which are critical in preventing cancer. p53 binds in a sequence-specific manner to DNA binding sites consisting of two decameric motifs or half-sites of the general form RRRCWWGYYY (R = A, G; W = A, T; Y = C, T) separated by 0–13 base pairs (El-Deiry et al., 1992; Funk et al., 1992). The p53 molecule consists of three major functional domains, of which the N terminus contains a transactivation domain, the core domain contains a sequence-specific DNA binding domain, and the C terminus incorporates oligomerization and regulatory domains (Ko and Prives, 1996; Levine, 1997; May and May, 1999).

The core domain of p53 is the main target for mutations, as 80%–90% of the missense mutations identified in human tumors are found in this region (Olivier et al., 2002). This underscores the importance of sequence-specific DNA binding by the core domain for the ability of p53 to function as a tumor-suppressor protein. Upon binding to DNA targets containing two half-site motifs, p53 forms tetramers, the protein's basic functional unit (Friedman et al., 1993; McLure and Lee, 1998; Nagaich et al., 1999; Wang et al., 1995; Waterman et al., 1995; Weinberg et al., 2004). Studies on DNA binding by p53 (Kaeser and Iggo, 2002; Resnick-Silverman et al., 1998; Szak et al., 2001; Thornborrow and Manfredi, 1999; Weinberg et al., 2005) and transcriptional activation (Inga et al., 2002; Qian et al., 2002) have shown that p53-dependent gene expression is encoded in the diverse sequences of its DNA target sites and in their relative arrangements. Hence, knowledge of the three-dimensional architecture of functional p53-DNA complexes has been highly sought after. The only structural information on p53 interaction with DNA published previously is based on the crystal structure of the DNA binding domain of human p53 bound as a monomer to a DNA duplex incorporating a single decameric motif. This study showed that the core domain adopts an immunoglobulin-like β sandwich that provides a scaffold for a DNA binding surface consisting of a loop-sheet-helix motif and two loops stabilized by a zinc ion (Cho et al., 1994). The crystal structure of the complex provided a starting framework for understanding the deleterious effects of naturally occurring mutations in the core region (Cho et al., 1994). However, the structural basis of DNA recognition by p53 tetramers and the mechanisms by which p53 recognizes different DNA targets remained unknown. Here, we have been able to obtain such functional structures by crystallizing p53 core domain with double-stranded DNA dodecamers incorporating different half-site motifs, (GGGCATGCCC, AGGCATGCCT, and GGACATGTCC). We show that each half-site binds two molecules of p53 in a sequence-specific manner, and two such dimers assemble into tetramers. We performed quantitative DNA binding studies on the various complexes, demonstrating that differential binding affinity in this series is correlated with sequence-specific variations in the protein-DNA contact geometry. The findings of the present study combined with earlier in vitro and in vivo data provide new insights into the mechanisms of p53 function and regulation.

Results and Discussion

Architecture of p53 Tetramers Bound to DNA

The core domain of human p53 used in the present study, referred to as the "core" or p53 DNA binding domain (p53DBD), spans residues 94–293. For

*Correspondence: bitali@techunix.technion.ac.il (T.E.H.); zippi.shakked@weizmann.ac.il (Z.S.)

Table 1. Crystal Structure Data and Refinement Statistics

Crystal Data/Complex	I	II	III	IV
DNA Sequence[a]	cGGGCATGCCCg (GGG)	aAGGCATGCCTt (AGG)	cGGACATGTCCg (GGA)	cGGACATGTCCg (GGA)
Space group	*P*1	*P*1	*P*1	*C*2
Unit cell (Å,°)	a = 54.5	a = 54.6	a = 54.5	a = 92.0
	b = 58.2	b = 58.0	b = 58.2	b = 67.9
	c = 77.6	c = 78.0	c = 77.5	c = 75.0
	α = 82.9	α = 83.4	α = 83.1	β = 93.0
	β = 88.0	β = 87.6	β = 88.0	
	γ = 73.6	γ = 73.5	γ = 73.6	
Volume ($Å^3$)	234,060	235,586	234,528	467,820
Protein molecules/ DNA duplexes in a.u	4/2	4/2	4/2	2/1
Resolution (Å)	40–1.8	43–2.2	40–1.85	38–2.5
Upper resolution shell (Å)	1.83–1.80	2.25–2.20	1.88–1.85	2.56–2.50
Measured reflections	690,667	431,843	741,598	140,547
Unique reflections	79,253	44,444	73,053	16,113
Completeness (%)	94.2 (90.6)[b]	96.2 (93.5)	93.9 (82.6)	99.9 (98.4)
$\langle I/\sigma(I)\rangle$	24.5 (4.0)	19.2 (5.7)	28.7 (3.5)	12.3 (2.9)
$R_{sym}(I)$ (%)	5.5 (34.2)	6.8 (25.5)	4.5 (35.0)	11.4 (44.3)
Refinement Statistics				
Number of reflections (I>0)	73,591	41,145	68,126	14,744
Working/test set	69,695/3896	38,957/2188	64,508/3618	13,971/773
R_{work}/R_{test} (%)[c]	15.3/21.7	14.5/21.5	16.2/22.5	16.4/25.1
Number of protein/ DNA/solvent atoms	6217/972/1054	6178/891/717	6144/912/998	3091/486/213
Average B factor ($Å^2$)	28.2	29.1	39.0	36.5
Rms deviation				
Bond lenghts (Å)	0.016	0.017	0.016	0.016
Bond angles (Å)	1.75	1.80	1.67	2.00

[a] The decameric motifs are capitalized.
[b] Numbers in parentheses correspond to the values in the upper resolution shell of data.
[c] $R = \Sigma h||Fobs(h)| - |Fcalc(h)||/ \Sigma h|Fobs(h)|$.

crystallization experiments, we used short oligonucleotides incorporating a single decameric motif. The best crystals of p53-DNA complexes were obtained with three DNA dodecamers that differ in their purine/pyrimidine tracts as follows: cGGGCATGCCCg, aAGGCATGCCTt, and cGGACATGTCCg (referred to as GGG, AGG, and GGA, lower-case letters signify nonconserved bases flanking the consensus decamer). The complexes with the three DNA sequences yielded isomorphous crystals (space group *P*1). The complex with the GGA target was also crystallized in a monoclinic crystal form (space group *C*2). The four crystal structures are referred to as I, II, III, and IV, respectively (Table 1).

In all crystal structures, four p53 core-domain molecules self-assemble on two B-DNA half-sites to form a tetramer made of a dimer of two identical dimers (referred to as *A-B* and *C-D* in Figure 1). The two B-DNA helices are stacked end to end, simulating a continuous double helix with two decameric half-sites separated by two base pairs. In each p53-DNA dimer, the two p53 molecules form sequence-specific contacts with symmetry-related regions of the decameric half-site and also interact with each other. Two such dimers associate into a tetramer via protein-protein and base-stacking interactions (Figure 1). The four protein-DNA interfaces within a tetramer are essentially identical, but they differ among tetramers depending on the specific DNA sequence (see below). The p53 core-domain tetramer and each of the two p53 core-domain dimers (referred to as the core tetramer and the core dimer, respectively) display symmetry coinciding with that of the DNA: a central dyad positioned between the DNA half-sites and a dyad within each half-site (Figure 1). In this configuration, the distance between the core dimers is ~35 Å, and they are rotated relative to each other by 33° in a clockwise manner, leading to propeller-like image of the core tetramer when viewed down the DNA helix axis (Figure 1C). This particular interdimer geometry is accommodated by DNA deformation and allows for protein-protein interactions between the core dimers along the DNA helix (Figure 1A). Although the current complexes between p53 tetramers and different DNA targets show a common overall architecture, variations in the assembly of dimers into tetramers are likely to occur when the DNA half-sites are contiguous or separated by a different number of base pairs.

The symmetry of the DNA bound core tetramer is distinctly different from that of the tetrameric structure formed by the oligomerization domain located at the C terminus of p53 (approximately residues 320–360) studied by NMR and X-ray crystallography (Clore et al., 1995; Jeffrey et al., 1995; Lee et al., 1994; Mittl et al., 1998). The C-terminal tetramer shows three global (bisecting) dyad axes perpendicular to each other, whereas the core tetramer has a single global dyad and two local ones at the two dimers. The structure of the core tetramer is intrinsic to the p53-DNA complex and is not induced by crystal symmetry, as three of the structures (I, II, and III) were

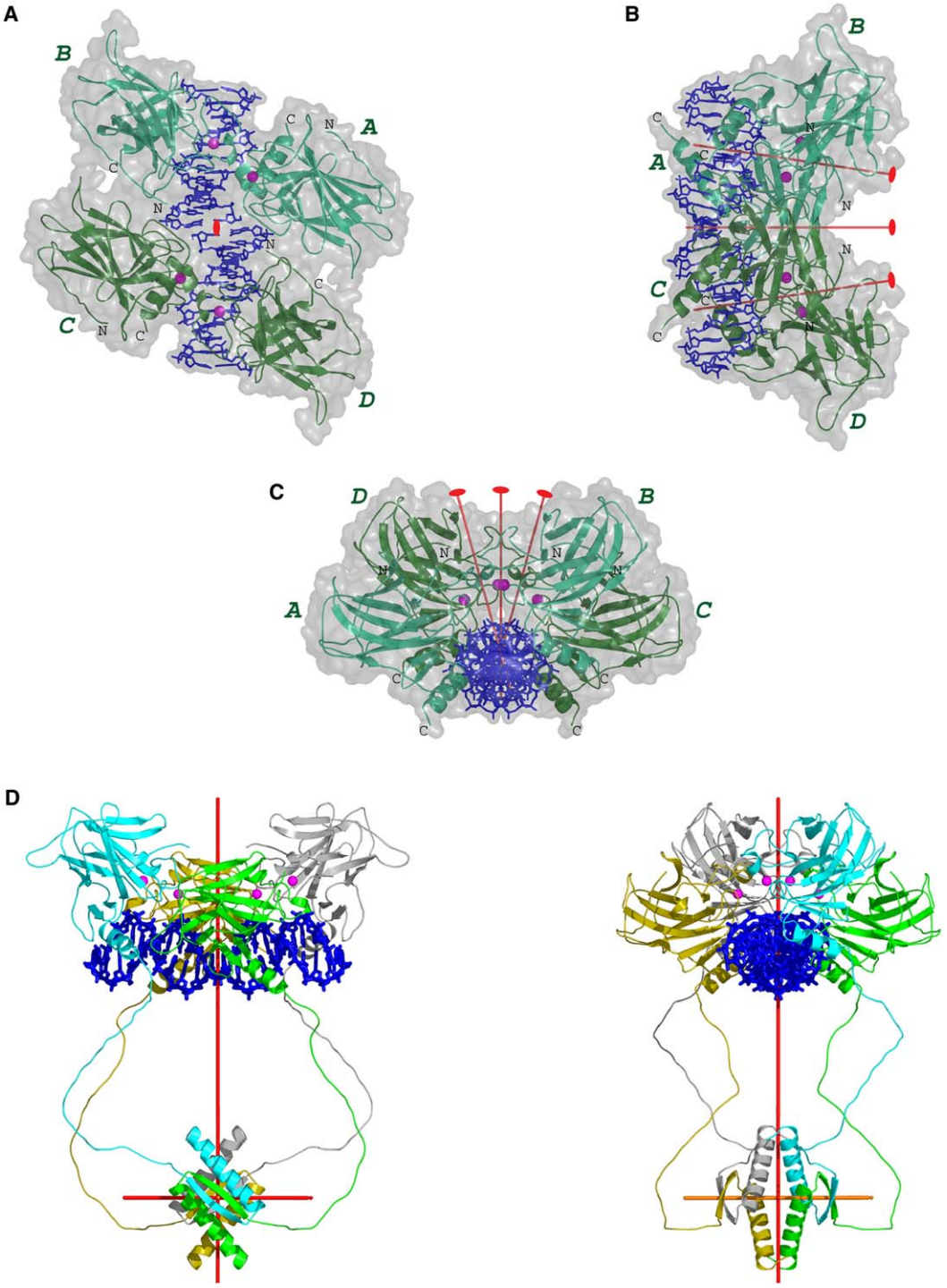

Figure 1. Different Views of p53 Tetramers Bound to DNA

Four p53 core domains (designated as *A*, *B*, *C*, and *D*) shown in ribbon representation interact with two double-stranded DNA half-sites (shown in blue). The core tetramer is a dimer of dimers: *A*-*B* (in cyan) and *C*-*D* (in green). Van der Waals surface of the complex is shown in transparent gray. The four Zn ions are shown as magenta spheres.

(A) View down the central dyad of the core tetramer.

(B) View perpendicular to the central dyad and the DNA helix axis.

(C) View down the DNA helix axis. The images are based on the monoclinic crystal structure (IV) that incorporates a crystallographic dyad. Also shown in red are the central dyad between dimers and the two local dyads within dimers.

(D) A model of p53 tetramer bound to DNA that incorporates the core and the oligomerization domains. The four molecules are shown in gold, gray, cyan, and green. Also shown in red are the three dyad axes of the C-terminal tetramer and the central dyad of the core tetramer. The two views are related to each other by a 90° rotation around the central dyad axis. Each of the four unstructured linkers between the two structured domains spans residues 291–326. The coordinates of the tetramerization domain are from Mittl et al. (1998) (PDB ID 1AIE). All structure-based figures were drawn by PyMol (DeLano, 2002).

obtained in a crystal form devoid of any symmetry. Importantly, the C termini of the four p53 core molecules point toward one face of the complex, whereas the N termini point toward the opposite face (Figures 1B and 1C). This geometry is compatible with the tetramerization of the full-length p53 molecule, as it allows the core tetramer to be spatially connected to the C-terminal tetramer via the linker region or hinge between the two domains. This is illustrated by the model in Figure 1D in which four unstructured chains (~30 residues long) link the C termini of the four core domains to the N termini of the four oligomerization domains. In this model, the central dyad of the core tetramer coincides with a dyad axis of the C-terminal tetramer, the one relating the two oligomerization dimers along their long dimensions. This is the only relative orientation between the two tetrameric domains that would lead to equal time-averaged distances between the ends of the four flexible chains, while maintaining the overall symmetry of the molecular assembly. The model highlights the mobile nature of p53 shown to contain large unstructured regions (Bell et al., 2002), and which appears to impede its crystallization. The observed self-assembly of p53 and DNA components in the crystal to generate tetrameric structures of the appropriate geometry and symmetry demonstrates their relevance to in vivo p53-DNA complexes.

Core-Domain Tetramers Are Stabilized by Protein-Protein Interactions

Two types of protein-protein interfaces are revealed by the p53 tetramers with a total buried surface area of nearly 2500 Å^2. The first one is located within each core dimer (*A-B* and *C-D* in Figure 1) and is referred to as the symmetrical interface. It is formed by residues of the H1 helix, the Zn cluster, and regions of the L2 and L3 loops from each core molecule illustrated in Figure 2. Overall views of the symmetrical dimer and the protein's secondary structure are in Figure S1 (in the Supplemental Data available with this article online). The buried area within each such dimer is rather modest, 600 Å^2, as also reflected by the narrow "waist" of the core dimer (Figure 2A). However, a combined network of hydrophobic and water-mediated polar interactions substantially stabilizes the core dimer as follows.

Two buried water molecules provide a central anchor for an internal hydrogen-bonding network that links the two Zn clusters and supports the relative configuration of H1 and L3. The core dimer is further stabilized by hydrophobic and polar interactions that can be grouped into several shells that surround the central hydration core. A shell of nonpolar interactions is formed by several surface residues positioned on the H1 helix and a large L3 hairpin: Pro177, His178, Met243, and Gly244. Two additional stabilization networks are observed next to the nonpolar layer. One is formed by charged residues from the two monomers (Arg181, Glu180, and Arg174) and several ordered water molecules stabilizing the dimer surface that is farthest from the DNA (Figure 2B). The second stabilization network is formed by the first-shell hydration of the protein surface facing the DNA minor groove supporting direct and water-mediated protein-DNA contacts formed by Ser241, Asn239, and Arg248 side chains. Thus, the ultimate "glue" of the dimer interface is provided by the DNA half-site. The involvement of several amino acids in the dimerization of the core domain upon DNA binding, discussed above, was also proposed on the basis of NMR studies (Dehner et al., 2005; Klein et al., 2001; Rippin et al., 2002) and mutagenesis/binding studies of the core domain (Dehner et al., 2005) and of the full-length p53 (Veprintsev et al., 2006). In addition, several polar and charged residues that are close to the protein surface, but not within the contact area, contribute to the stability of the interacting monomers via hydrogen bonds, salt bridges, and water-mediated interactions. In particular, bidentate salt bridges on opposite sides of each p53 monomer formed by Asp184 with Arg175 and by Arg249 with Glu171 support the integrity of the core dimer (Figures 2A and 2B). It is noteworthy that a large number of surface amino acids that contribute to dimer stability or to DNA binding were shown to be involved in protein-protein interactions with 53BP1 and 53BP2 implicated in DNA damage response and apoptosis, respectively (Derbyshire et al., 2002; Gorina and Pavletich, 1996; Joo et al., 2002). Such interactions would impede the dimerization of p53 core domains on DNA observed here. Hence, it is likely that p53 activation by the apoptosis-stimulating protein ASPP2, via its interaction with the 53BP2 region of ASPP2 (Samuels-Lev et al., 2001), involves alternative forms of core-DNA assemblies that are critical for the selection of proapoptotic promoters.

The symmetrical dimer is stabilized by evolutionary-conserved surface amino acids (Dehner et al., 2005; Walker et al., 1999). All the residues that support the dimerization interface discussed above were shown to be mutated in human cancer (Olivier et al., 2002), thus pointing to their functional role in contributing to the integrity and stability of p53 oligomers bound to DNA as well as mediating interactions with other proteins. These residues include four of the most frequently mutated codons or hot spots, namely Arg175, Gly245, Arg248, and Arg249. Gly245 is essential for "shaping up" the L3 hairpin at the protein-protein interface, whereas R175 and R249 support the two large loops, L2 and L3, as described above. R248 plays a key role in docking the symmetrical core dimers to their DNA half-sites (see also below). However, unlike the universality of the symmetrical protein-protein interface, which is robust and conserved among the various complexes, the other type of interface that is formed between dimers shows a certain level of variability. This kind of interface, referred to as the translational interface (*B-C* or *A-D* in Figure 1 and in Figures S2 and S3) links the two core dimers along each side of the DNA helix. The translational interface is likely to be modulated by the DNA target as well as by interacting proteins, thus providing another level of regulation in p53 activity.

Binding Cooperativity and Functional Implications for Modified p53 Proteins

The present findings provide a structural basis for understanding observations on DNA binding and transcriptional activation by p53 variants. It was shown that p53 segments including the tetramerization region exist in solution mainly as dimers and bind DNA mostly as tetramers, whereas p53 proteins devoid of the tetramerization domain are mostly monomeric in solution but

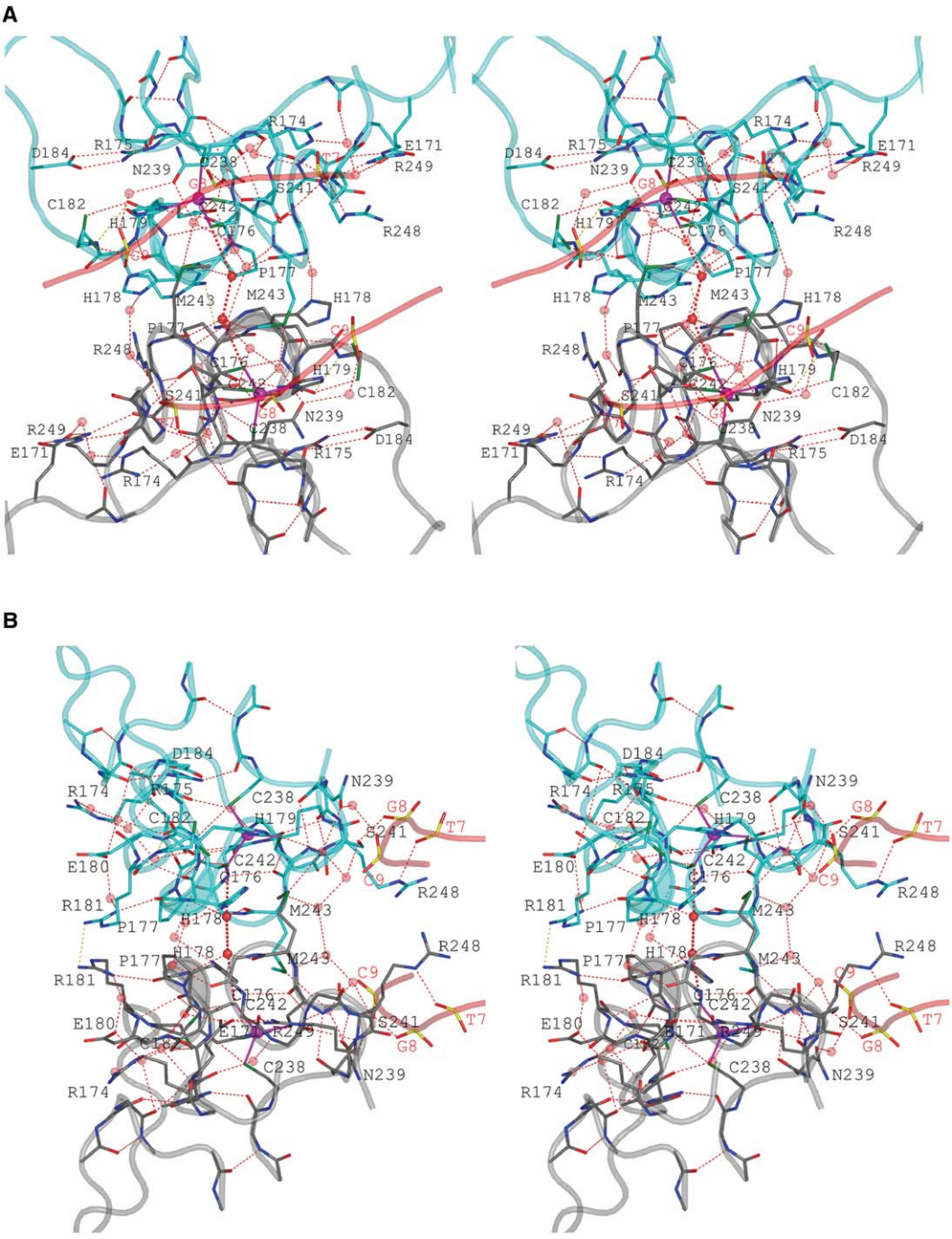

Figure 2. Stereo Views of the Symmetrical Protein-Protein Interface

(A) View down the dyad axis of the dimer.

(B) View perpendicular to that dyad. These are based on the core dimer of complex I. The protein regions from the two core molecules are shown in cyan and gray with the corresponding ribbon representation. The DNA backbone and nucleotide labeling are shown in light red. Zn ions are shown as magenta spheres. Water atoms are shown as transparent red spheres. The central hydration is highlighted by solid spheres.

form tetramers with DNA targets incorporating two decameric repeats (e.g., Weinberg et al., 2004). These findings suggested that the cooperative binding of p53 to DNA is supported by protein-protein interactions via the core domain (Weinberg et al., 2004). The present structures show that the core tetramer is stabilized by protein-protein interactions within each dimer as well as between dimers. We propose that such interactions are critical in stabilizing functional p53-DNA complexes in cases in which specific DNA interactions are diminished as a result of truncated core domains found recently in alternatively spliced isoforms of human p53 (Bourdon et al., 2005; Rohaly et al., 2005). The Δp53 isoform identified by Rohaly et al. (2005) has a 66 residue deletion (257–322) compared to the regular protein. Yet, Δp53, lacking part of the core domain and the hinge

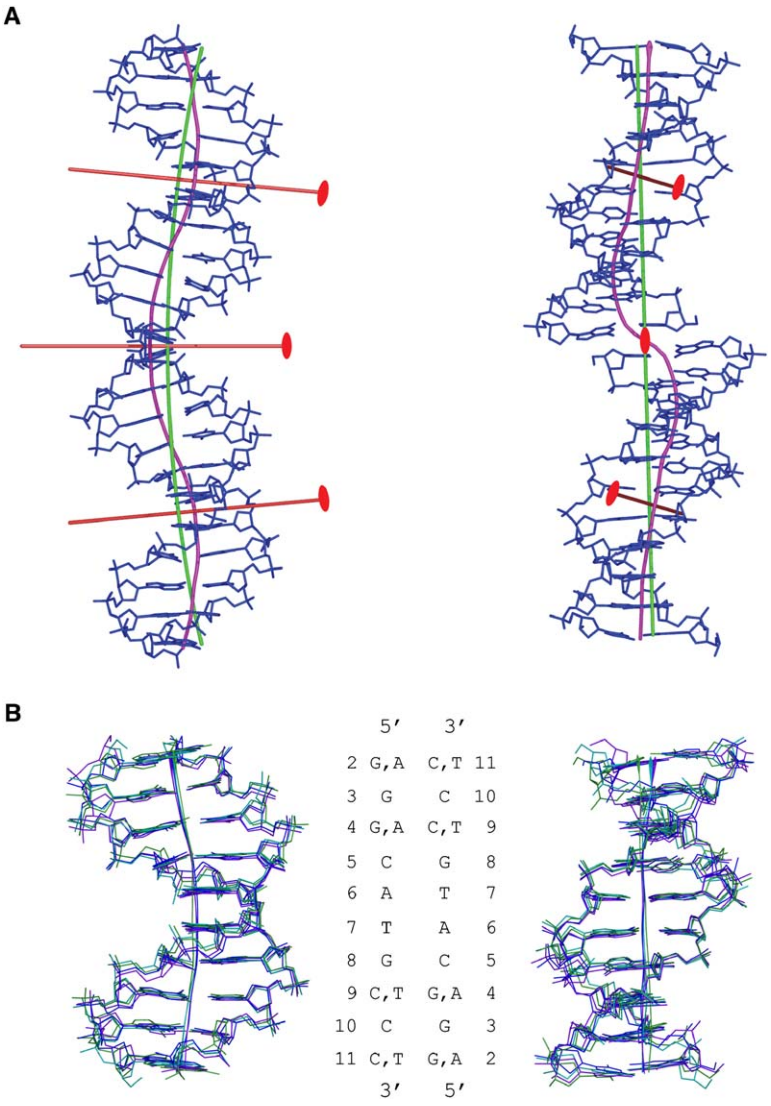

Figure 3. DNA Trajectories

(A) Two stacked DNA half-sites of cGGACA TGTCCg from the symmetrical p53-DNA complex (IV). The c/g base pairs at each end of the 24 base pair DNA are frayed and are not shown. Also shown are the global curved helix axis (in magenta) derived by CURVES (Lavery and Sklenar, 1989), the best fitted arc in green (Slickers et al., 1998), and the global and local dyad axes in red. Views are perpendicular to the central dyad axis (left) and down that dyad (right).

(B) Superposition of DNA decameric half-sites (one from each of the four p53-DNA complexes) with their global helix axes shown in cyan (I), green (II), purple (III), and blue (IV). Views are perpendicular to the decamer dyad (left) and down that dyad (right). Also shown are the base sequences and numbering scheme.

region, can associate with and transactivate certain p53-inducible promoters. It is likely that Δp53 can bind to specific DNA targets as a tetramer (even in the absence of several protein-DNA interactions) because the regions that contribute to core-core interactions are intact in this p53 isoform. Several other isoforms, truncated at the N terminus, the C terminus, or both termini in comparison to regular p53, were shown to be expressed in normal human tissue in a tissue-dependent manner (Bourdon et al., 2005). Whereas one variant (p53β), lacking the tetramerization domain (residues 331–393), was shown to enhance p53 target gene activation in a promoter-dependent manner, another variant (Δ133p53), lacking the transactivation domain and part of the core domain (residues 1–132), was shown to inhibit apoptosis mediated by full-length p53. These p53 variants could form protein-DNA assemblies of the geometry shown here by the p53 core tetramers, albeit of reduced affinity and stability in comparison to regular p53. The dominant-negative effect of Δ133p53 could result from its heterooligomerization with full-length p53, thereby inhibiting both its DNA binding and transactivating capabilities.

DNA Conformation

The palindromic DNA targets (GGG, AGG, and GGA) used here differ in their purine/pyrimidine sequences. In all complexes, two dodecamers are stacked end to end, simulating a continuous double helix (Figure 3A). The stacking geometry at the junction between dodecamers is sequence dependent. In the case of the AGG dodecamer, the nonconserved stacked t/a base pairs display the Hoogsteen base-pairing geometry instead of the Watson-Crick geometry displayed by the stacked g/c base pairs of the other dodecamers. However, the global DNA conformation is similar for the various structures. Superposition of decameric half-sites from the four crystal structures shows that the common CATG region at the center is very similar among the different crystal structures, whereas the flanking regions show some significant variations in their local conformations, depending on the specific base sequence (Figure 3B).

A remarkable feature of the p53-DNA assemblies is the organization of the two DNA half-sites within the tetramer. The DNA trajectory is highlighted in Figure 3A by the global curved helix axis (magenta), the best fitted arc (green), and the three DNA dyads (red): two dyads within

the half-sites and one between them. The global DNA axis has a snake-like shape displaying a sharp kink at the junction between the two dodecamers (see details in Supplemental Data). The DNA trajectory demonstrates that each of the decameric half-sites is bent toward its major groove and away from the core dimer, in accordance with gel-based phasing analysis of similar half-sites bound to p53 (Nagaich et al., 1999). However, the combined two half-site DNAs separated by two base pairs are slightly bent toward the core tetramer (Figures 1B and 3A). This unique deformation appears to optimize both protein-DNA and protein-protein interactions within the tetrameric complex.

Structural Basis of Differential DNA Recognition by p53

The protein-DNA interface in the various complexes is held primarily by residues from the loop-sheet-helix motif (L1, S10, and H2) and the L3 loop as observed for the monomeric p53-DNA complex (Cho et al., 1994). However, striking alterations in the DNA recognition pattern depending on the base sequence, as well as water-mediated interactions that contribute to the integrity of the protein-DNA interface, are revealed by the current high-resolution structures.

Direct contacts between p53 side chains and the DNA bases are made by four amino acids within the major groove of each pentameric duplex or quarter-site: Arg280, Lys120, Ala276, and Cys277 (Figures 4A, 4B, and 5). Direct contacts to the DNA backbone are formed by Ser241 and Arg273 and occasionally by Arg248 as well as by the backbone amides of Lys120 and Ala276 (Figures 4A, 4B, and 5). Arg280 plays a major role in anchoring p53 to the DNA major groove via two direct hydrogen bonds to the highly conserved guanine base (G8). These interactions and four contacts to the DNA backbone are supported by an extensive network of hydrogen bonds involving the side chains of Asp281 and Arg273, the backbone atoms of Ala276 and Cys277, and a highly conserved water molecule making four optimally oriented hydrogen bonds (Figures 4A and 4B). Arg273 residues play a pivotal role in docking p53 to the DNA backbone at the central region of each half-site where no base-mediated contacts exist. Substitution of Arg273 by His273 or Cys273, which are highly abundant in human tumors (being one of the six hot spots), leads to a dramatic reduction in the DNA binding affinity, even though the protein retains a wild-type stability (Bullock and Fersht, 2001).

In contrast to the contact geometry shown by Arg280 and the buttressing residues that are invariant among the different DNA targets, the specific interactions formed by the three other amino acids (Lys120, Ala276, and Cys277) change dramatically when the central base pair of the pentameric quarter-site is changed from G/C to A/T (illustrated in Figures 4 and 5). In the first case, Lys120 makes two or three hydrogen bonds with successive guanine bases (G3 and G4), and C277 interacts with C9 base of the opposite strand (Figure 5). However, in the second case, Lys120 interacts with G3 and T9 bases from opposite strands, whereas Cys277 is involved in van der Waals interaction with T9. Yet, the most striking change in the contact geometry is a hydrophobic interaction formed between the methyl group of Ala276 and the methyl group of the T9 base. To enable this favorable interaction, the A/T base pair at the center of the pentamer and the preceding G/C pair are moved away from the protein in comparison to the corresponding G/C base pairs of the other targets (Figure 4C). This kind of local deformation in the DNA helix ("indirect readout") allows for optimizing direct protein/DNA interactions ("direct readout"), as shown here. Such sequence-specific direct and indirect readout mechanisms account for differential DNA binding affinity shown by p53 (see below).

The largest diversity in protein-DNA interactions is displayed by Arg248 residues that anchor the p53 core domain to the DNA at the minor groove side. They show a wide range of conformations from folded to fully extended side chains. Most of the interactions made by Arg248 are not within the DNA quarter-site contacted by the other amino acids of the same molecule but at the adjacent quarter-site. In the various complexes, the side chains of Arg248 support the DNA minor groove hydration, forming an integral part of the extended solvent network that links the p53 core dimers to their DNA half-sites (as exemplified by the GGA complex in Figure S5). Thus, Arg248 residues, embracing the DNA from the minor groove side, support the integrity and stability of the core dimers bound to their DNA half-sites. Mutations in this codon (being one of the six p53 hotspots) to Gln248 or Trp248 that are highly abundant in human cancer would disrupt the integrity of the core dimers bound to DNA, resulting in p53 dysfunction.

A comparison of the recognition patterns displayed by the different DNA binding sites demonstrates that the stringent requirement in the decamer sequence is the conserved C/G base at the fourth position from each end followed by a purine/pyrimidine base at the third position. These bases play a major role in the stabilization of the protein-DNA interface with the robust interaction made by Arg280 and the alternative modes shown by Lys120, Ala276, and Cys277 depending on the identity of the bases: G/C versus A/T. Changes from the consensus sequence, without a significant reduction in the binding affinity, can be envisaged at the second position of the decamer, due to the ability of Lys120 to act as a hydrogen bond donor to either stacked bases or diagonally positioned bases observed here and in other structures (Luscombe et al., 2001). The identity of the bases at each end of the decamer appears to be less important than that of the above three sites, as this base is not involved in any direct interaction with the protein. The A/T base-pair doublet at the center of each decameric half-site is involved only in water-mediated interactions, yet it plays an essential role in the cooperative binding of the core dimer to its DNA half-site through minor groove hydration. Also, variations in this base-pair doublet and the others can contribute to indirect readout effects by tuning the flexibility and hence the energetic cost required to bend the DNA helix in its complex with the protein (see below).

DNA Binding Affinity Is Modulated by Both Direct and Indirect Readouts

The DNA binding affinities of the core domain as a function of the DNA binding sites used in the crystal structures were determined by a quantitative electrophoretic

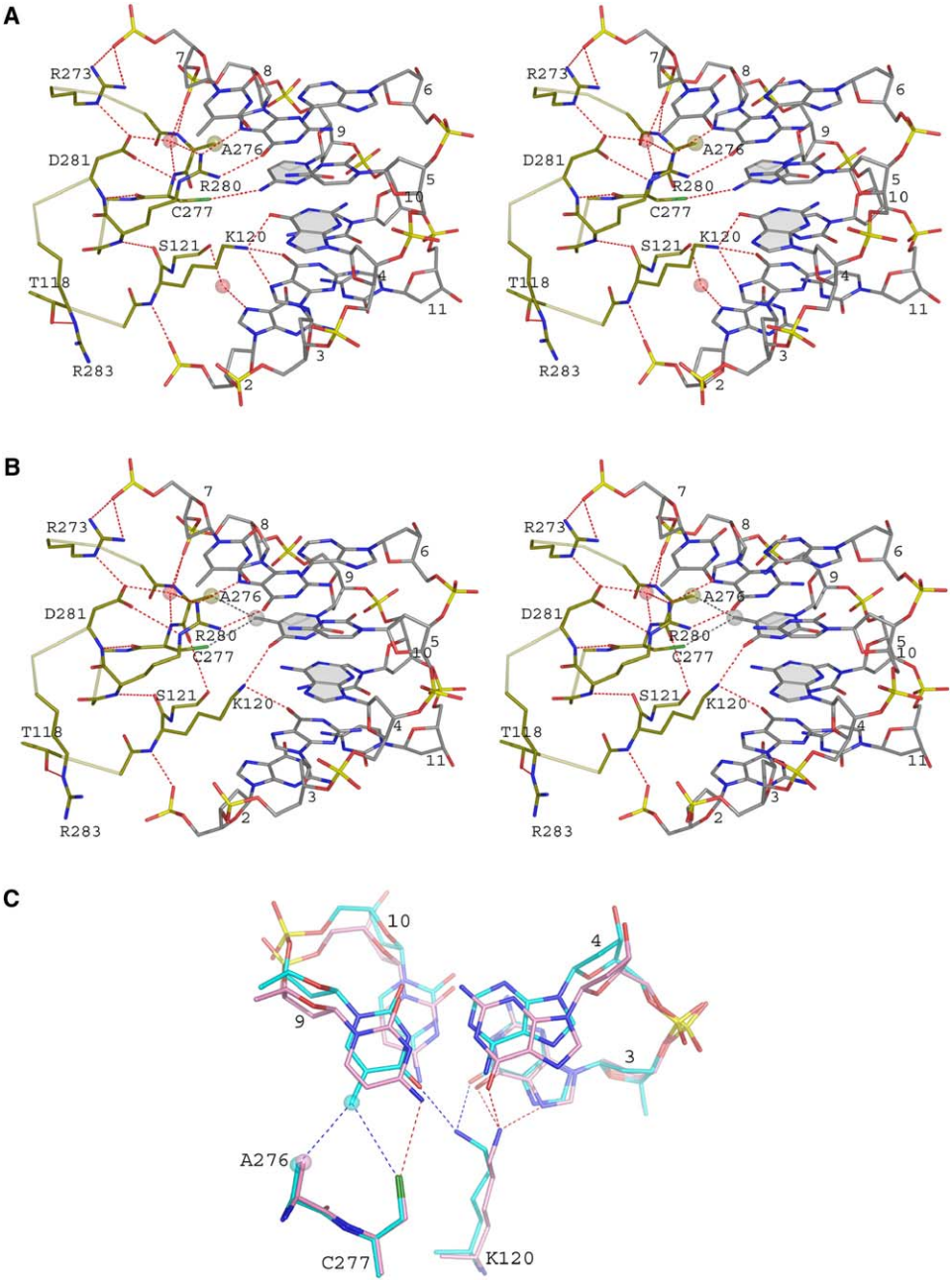

Figure 4. DNA Recognition by p53

(A) p53 interaction with GG**G**CA/TG**C**CC (complex I).

(B) p53 interaction with GG**A**CA/TG**T**CC (complex III). Nucleotide numbering (5′–3′ direction) is from 2 to 6 for the first strand and from 7 to 11 for the second strand. All-atom views are shown for the DNA and only relevant residues for p53. The central base pair for each pentamer is highlighted. The methyl groups of Ala276 and of the T9 base are shown as transparent spheres.

(C) Comparison between the central recognition patterns of p53 bound to GGG or GGA targets. C atoms are shown in pink and cyan, respectively. Other color codes are red, blue, green, and yellow for O, N, S, and P atoms, respectively. Hydrogen bonds and other interactions are shown as broken lines in red and blue, respectively. The methyl groups are shown as large transparent spheres.

mobility shift assay (see Experimental Procedures). Two types of DNA binding sites were used, with the decameric repeats (GGG, AGG, or GGA) being either contiguous or separated by two base pairs. The gel shifts of the various binding sites and the corresponding dissociation constants are shown in Figure 6. The overall dissociation constants for the "contiguous" DNA targets range from 14 to 50 nM. The two base-pair insertion between decamers of each binding site leads to lower affinities, the corresponding values ranging from 20 to 84 nM. The reduced binding affinity can be attributed to indirect effects associated with DNA deformation at the junction between half-sites. Moreover, these complexes are of lower stability, as indicated by the smeared gel shifts, probably due to weaker stabilizing interactions between the p53 dimers. The highest binding affinity in this

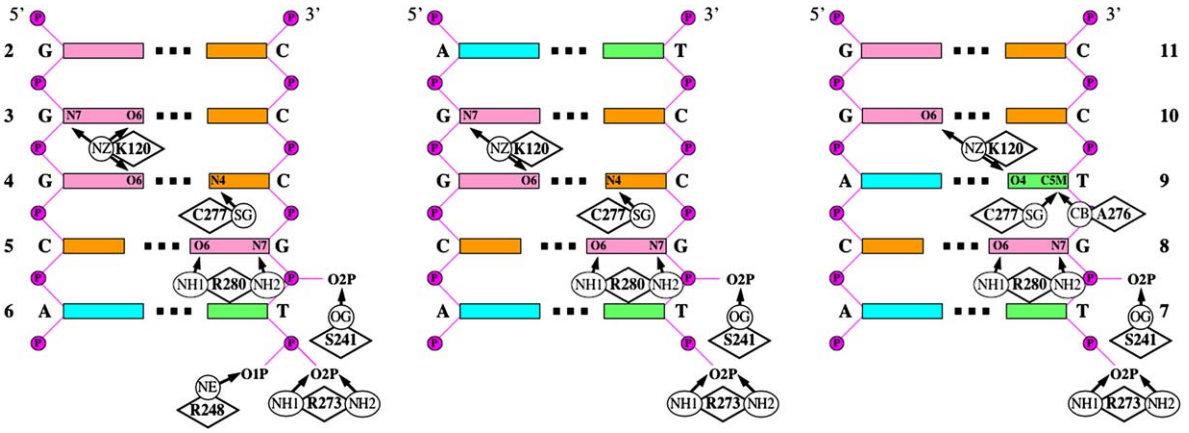

Figure 5. Schematic Representation of Protein-DNA Interactions in the Different Complexes

Direct interactions between p53 side chain atoms and the DNA bases or backbone atoms are shown by arrows. Only one pentameric duplex is shown for each complex, as the other ones are related by symmetry. From left to right are GGGCA/TGCCC (complex I), AGGCA/TGCCT (complex II), and GGACA/TGTCC (complexes III and IV). Direct contacts to DNA by Arg248 side chains within the same quarter-site are observed only for one core dimer in complex I (shown here and in Figure 2). All other contacts involving Arg248 are via water molecules (see text).

series is shown by the GGA targets and can be rationalized by the favorable hydrophobic interaction between Ala276 side chain and the thymine methyl group at each of the four quarter-sites as described above. The lowest binding affinities displayed by the AGG targets should be attributed to indirect readout effects, as the first base pair at each decameric end is not involved in direct interactions with the protein.

The present findings provide a structural basis for understanding differential DNA binding by natural p53 binding sites. Systematic studies of such targets have shown that DNA response elements involved in cell-cycle arrest, incorporating "permissible" deviations from the consensus sequence (according to the contact-based criteria discussed above), displayed the highest affinity for p53, whereas several of the lowest-affinity targets, displaying "nonpermissible" deviations, were those involved in apoptosis in agreement with transcriptional activation data (Qian et al., 2002; Weinberg et al., 2005). Moreover, a refined consensus sequence of p53 binding sites obtained from chromatin immunoprecipitation experiments together with paired-end ditags sequencing strategy (Wei et al., 2006) can be rationalized by our structural and DNA binding data. In particular, the base observed most frequently at the third position from each end is A/T. This corresponds to the present GGA binding site, shown here to be the target of the highest binding affinity as a result of the hydrophobic interaction involving the thymine base.

A Model for Full-Length p53 Bound to DNA and Implications for p53 Function and Autoregulation

The p53 molecule contains the three major domains common to classical transcription factors, namely a transactivation domain, a sequence-specific DNA binding domain, and an oligomerization domain. However, it is unique among other transcription factors in having an additional domain at its extreme C terminus shown to bind in a sequence nonspecific manner to a wide variety of DNA targets including double and single-stranded DNA as well as unusual DNA structures (reviewed by Jayaraman and Prives [1999], Kim and Deppert [2006]). The role of the extreme C-terminal domain (CTD) in p53 function has been highly controversial for over a decade. Several studies proposed that sequence-specific DNA binding by p53 is negatively regulated by the CTD (reviewed by Ahn and Prives [2001]), whereas others implied that this domain has no effect on this activity (Espinosa and Emerson, 2001; Kaeser and Iggo, 2002; Wolcke et al., 2003). Recently, evidence supportive of positive regulation by the CTD was published (Liu et al., 2004; McKinney et al., 2004). Here we propose a model for full-length p53 bound to DNA and a unified structure-based mechanism that explains the different regulatory effects of the CTD on p53 function.

The binding of four p53 core domains to DNA imposes a unique stereochemistry on this system, in which the four C termini of the core domains point toward one face of the complex, whereas the four N termini point toward the opposite face, as described above. This stereochemistry determines the three-dimensional architecture of the full-length p53 molecule bound to its DNA target as illustrated by the cartoon in Figure 7A based on the structural model of Figure 1D. The two structured domains (core and oligomerization) are separated by four flexible chains (shown as dotted lines in Figure 7). In this arrangement, two CTD chains are close to the DNA, and the other two are distant from the DNA, referred to as the "proximal" CTD and the "distal" CTD, respectively (shown as curved arrows in Figure 7). Based on this model, we propose that an additional stabilization of the sequence-specific complex of p53 with DNA is achieved by nonspecific electrostatic interactions between the positively charged proximal CTD and the DNA backbone. Quite remarkably, it appears that the system is especially designed for such supporting interaction via the CTD, because the DNA helix facing the proximal CTD from its minor groove side (Figures 1D and 7A) as well as the adjacent phosphate oxygens on either side are not involved in any contacts with the core domain residues and are freely disposed to interact with the proximal CTD chains. In this way, the proximal CTD helps to "dock" the DNA onto the core tetramer

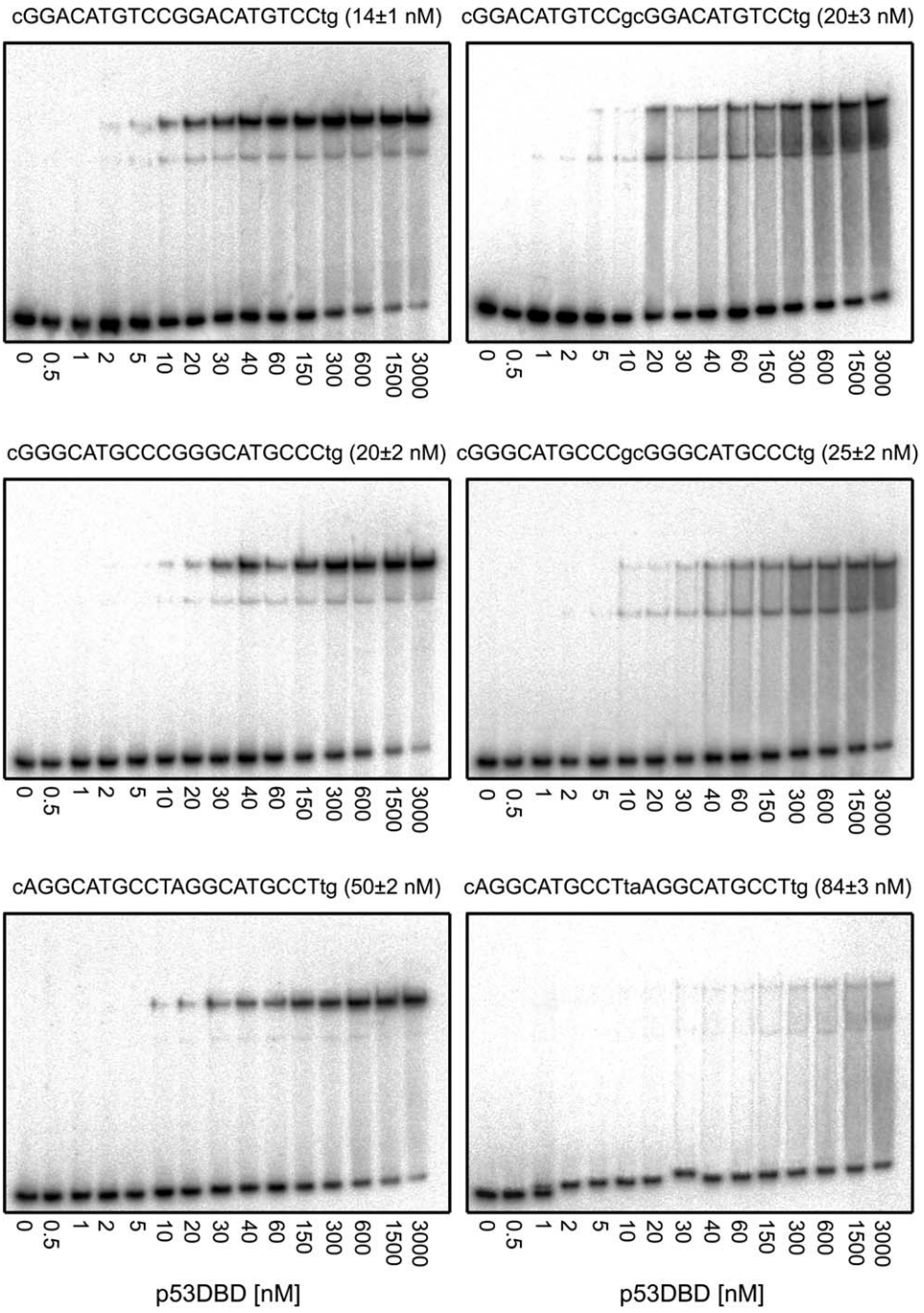

Figure 6. Binding Affinity Measurements of p53DBD/DNA Complexes

Gels showing representative results for the binding affinity of p53DBD to DNA targets embedded in hairpin constructs (50 pM). Upper bands show protein bound DNA, and lower bands show unbound DNA. The numbers below each gel show the concentration of p53DBD monomers active for DNA binding. Lowercase letters refer to nonconserved bases flanking each decameric repeat. The dissociation constants and their standard errors (nM) are shown next to the sequence of each binding site.

and hence positively regulate p53 binding to its DNA response elements, leading to enhanced transcriptional activation as reported (Liu et al., 2004; McKinney et al., 2004).

In the cell, p53 has to identify and bind to its specific DNA targets in the context of a large excess of nonspecific DNA. Clearly, such a search would involve frequent binding to nonspecific DNA. Based on the structural data, we propose that several amino acids of the core domain that are involved in direct binding to specific DNA binding sites could also contribute to the affinity of complexes with nonspecific double-stranded DNA. These include the side chains of Gln239, Ser241, Arg248, Arg273, and Asp281 and the backbone amides of Lys120 and Ala276, all interacting with the DNA backbone, either directly or through water molecules. Hence,

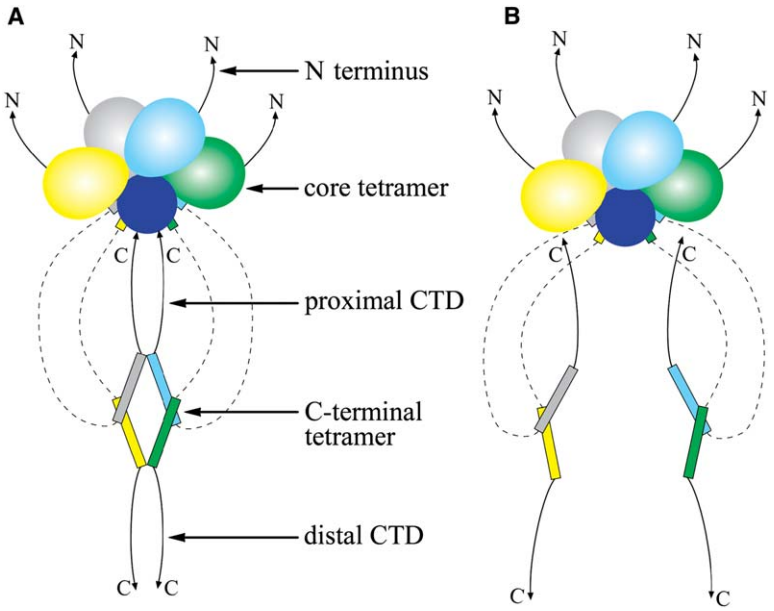

Figure 7. A Model for Full-Length p53 Tetramer Bound to DNA

The model is based on the structural model of Figure 1D.

(A) Closed complex where the core tetramer and the oligomerization tetramers are both intact.

(B) Partially opened complex where the C-terminal tetramer is dissociated into two dimers. The core-domain tetramer is shown as four colored balloons with four squared tips for the C termini. The oligomerization tetramer is shown as four elongated rectangles, each representing the long α helix and the short β strand of this domain. The color code is as for Figure 1D. The unstructured chains connecting the two tetramers are shown as dotted lines, and the extreme C-terminal domains (CTDs) are shown as curved arrows.

p53 has the potential to form high-affinity complexes with nonspecific DNA as observed previously (Wolcke et al., 2003). If p53 uses both the core domain and the CTD for binding to either specific or nonspecific DNA targets, as proposed here, then an excess of nonspecific DNA in *trans* with the binding site (i.e., on separate long DNA) would lead to inhibitory effects on sequence-specific DNA binding. Such effects can be alleviated by various CTD modifications (reviewed by Ahn and Prives [2001]) that appear to significantly lower the binding affinity of p53 to nonspecific DNA relative to sequence-specific DNA. However, if the competing sequence is in *cis* with the binding site (i.e., on the same DNA), the CTD could facilitate the protein's search for its cognate DNA shown by McKinney et al. (2004) and Liu et al. (2004) (see discussion below). In addition to the proximal CTD, the distal CTD can further support p53-DNA complexes, particularly when such interactions involve DNA looping. DNA looping mediated by the distal CTD can also bring into close proximity other transcriptional activators that work in synergy with p53.

Two major pathways were proposed for proteins searching the genome for their sequence-specific sequences: a one-dimensional mechanism referred to as linear diffusion, in which the protein slides along the DNA helix while maintaining continuous contact with the DNA; and a three-dimensional pathway either through rapid dissociation/reassociation events or via "intersegment transfer" processes in which the protein moves from one DNA segment to another without losing contact with the DNA (reviewed by von Hippel and Berg [1989]). McKinney et al. (2004) have shown that p53 is capable of linear diffusion mediated by the CTD. Our model shows how p53 can efficiently search the DNA for its target sites, at least for short DNA distances. In the present configuration, the DNA helix is "locked" by four p53 molecules, with the core tetramer at one end and the proximal CTD with the attached C-terminal tetramer on the other, as well as by the surrounding flexible chains connecting the two tetramers. Releasing the DNA for a three-dimensional search through the dissociation of the C-terminal tetramer into two dimers (Figure 7B) appears more probable than releasing the DNA via the dissociation of the core tetramer because the latter is held by both protein-protein and protein-DNA interactions. However, DNA release toward the C terminus would involve electrostatic trap, first by the proximal CTD and then by the distal CTD. Hence, linear diffusion of p53 along the DNA maintaining continuous contact with the DNA backbone via the CTD would be facilitated by the unique architecture of the p53 tetramer. Clearly, the deletion of the CTD would greatly ease the release of DNA from its p53 "confinement" and thus hamper p53 sliding as reported (McKinney et al., 2004).

Here we focused on the possible regulatory effects of the extreme CTD on p53 function. However, in addition to the CTD, a region located within the acidic N terminus was shown to negatively regulate DNA binding (Cain et al., 2000). According to our structure-based model, the four N termini are directed toward the tetramer face distant from the DNA (Figure 7). On the one hand, the proximity of the four N termini is expected to destabilize the core tetramer due to electrostatic repulsion between the negatively charged chains, leading to increased dissociation from the DNA relative to p53 lacking the N terminus as shown by Cain et al. (2000). On the other hand, the common orientation of the four N termini could facilitate the recruitment of coactivators that act in a cooperative manner in mediating the transcription of p53-resposive genes (An et al., 2004). Future structural studies of p53 interaction with DNA and with partner proteins together with the relevant in vitro and in vivo experiments will provide further insights into the intricate molecular mechanisms employed by p53 in its function as the guardian of the genome.

Experimental Procedures

Protein and DNA Production

The DNA sequence encoding the human p53 core domain or p53DBD (residues 94–293) was subcloned into pET-27b (Novagen). The plasmid was transformed into *E. coli* BL21 (DE3) strain. Protein

production was conducted following a procedure published for the mouse p53DBD (Zhao et al., 2001). Synthetic DNA oligonucleotides were purified by reverse-phase high-pressure liquid chromatography (see Supplemental Data).

Crystallization and X-Ray Analysis

Complexes between p53DBD and various DNA targets were prepared by mixing the protein solution with the DNA solution (20% molar excess of DNA). The best crystals were obtained by vapor diffusion with PEG/Ion solutions from complexes with three different DNA dodecamers (Table 1). X-ray diffraction data from each crystal, flash cooled at 100 K, were measured on a Rigaku R-AXIS IV++ detector mounted on a RIGAKU RU-H3R generator with CuKα radiation focused by Osmic confocal mirrors. The data were processed with DENZO/SCALEPACK (Otwinowski and Minor, 1997). The structures were solved by CNS (Brunger et al., 1998) and refined by CNS and REFMAC (Murshudov et al., 1997). Crystal structure data and refinement statistics are in Table 1. Additional details on crystallization conditions, data collection, and analysis are given in Supplemental Data.

DNA Binding Studies

Synthetic DNA sequences were purified by reverse-phase cartridge. The sequences were designed as intramolecular hairpin constructs, with either 23 bp in the stem (for molecules containing two abutting decameric repeats) or 25 bp in the stem (for molecules containing two decamers separated by two base pairs), and with five cytosines in the loop. The advantage of intramolecular hairpins for DNA binding studies was previously discussed (Haran et al., 1992). Although it appears that binding in this system proceeds through dimers and then tetramers or vice versa (Figure 6), the analysis by a two binding site model is complicated by the instability of the complexes and cannot be parsed correctly. Hence, we analyzed the gels only for the overall reaction. For details, see Supplemental Data.

Supplemental Data

Supplemental Data include five figures, one table, Supplemental Experimental Procedures, Supplemental Results and Discussion, and Supplemental References and can be found with this article online at http://www.molecule.org/cgi/content/full/22/6/741/DC1/.

Acknowledgments

We thank our colleagues Y. Halfon, R. Rohs, L. Shimon, M. Eisenstein, Y. Diskin, O. Suad, and F. Frolow for help and discussion; D.M. Crothers, B. Honig, M. Oren, and A. Minsky for comments to the manuscript; and A.R. Fersht for communication of data prior to publication. This work was supported by grants from the Kimmelman Center for Macromolecular Structure and Assembly, the Philip M. Klutznick Research Fund, and the EC (FP6) program (to Z.S.) and the Israel Science Foundation and Israel Cancer Association (to T.E.H.). This publication reflects the authors' views and not necessarily those of the EC. The community is not liable for any use that may be made of the information. Z.S. holds the Helena Rubinstein professorial chair in Structural Biology.

Received: February 10, 2006
Revised: April 18, 2006
Accepted: May 10, 2006
Published: June 22, 2006

References

Ahn, J., and Prives, C. (2001). The C-terminus of p53: the more you learn the less you know. Nat. Struct. Biol. *8*, 730–732.

An, W., Kim, J., and Roeder, R.G. (2004). Ordered cooperative functions of PRMT1, p300, and CARM1 in transcriptional activation by p53. Cell *117*, 735–748.

Bell, S., Klein, C., Muller, L., Hansen, S., and Buchner, J. (2002). p53 contains large unstructured regions in its native state. J. Mol. Biol. *322*, 917–927.

Bourdon, J.C., Fernandes, K., Murray-Zmijewski, F., Liu, G., Diot, A., Xirodimas, D.P., Saville, M.K., and Lane, D.P. (2005). p53 isoforms can regulate p53 transcriptional activity. Genes Dev. *19*, 2122–2137.

Brunger, A.T., Adams, P.D., Clore, G.M., DeLano, W.L., Gros, P., Grosse-Kunstleve, R.W., Jiang, J.S., Kuszewski, J., Nilges, M., Pannu, N.S., et al. (1998). Crystallography & NMR system: a new software suite for macromolecular structure determination. Acta Crystallogr. D Biol. Crystallogr. *54*, 905–921.

Bullock, A.N., and Fersht, A.R. (2001). Rescuing the function of mutant p53. Nat. Rev. Cancer *1*, 68–76.

Cain, C., Miller, S., Ahn, J., and Prives, C. (2000). The N terminus of p53 regulates its dissociation from DNA. J. Biol. Chem. *275*, 39944–39953.

Cho, Y., Gorina, S., Jeffrey, P.D., and Pavletich, N.P. (1994). Crystal structure of a p53 tumor suppressor-DNA complex: understanding tumorigenic mutations. Science *265*, 346–355.

Clore, G.M., Ernst, J., Clubb, R., Omichinski, J.G., Kennedy, W.M., Sakaguchi, K., Appella, E., and Gronenborn, A.M. (1995). Refined solution structure of the oligomerization domain of the tumour suppressor p53. Nat. Struct. Biol. *2*, 321–333.

Dehner, A., Klein, C., Hansen, S., Muller, L., Buchner, J., Schwaiger, M., and Kessler, H. (2005). Cooperative binding of p53 to DNA: regulation by protein-protein interactions through a double salt bridge. Angew. Chem. Int. Ed. Engl. *44*, 5247–5251.

DeLano, W.L. (2002). The PyMOL Molecular Graphics System (San Carlos, California: DeLano Scientific).

Derbyshire, D.J., Basu, B.P., Serpell, L.C., Joo, W.S., Date, T., Iwabuchi, K., and Doherty, A.J. (2002). Crystal structure of human 53BP1 BRCT domains bound to p53 tumour suppressor. EMBO J. *21*, 3863–3872.

El-Deiry, W.S., Kern, S.E., Pietenpol, J.A., Kinzler, K.W., and Vogelstein, B. (1992). Definition of a consensus binding site for p53. Nat. Genet. *1*, 45–49.

Espinosa, J.M., and Emerson, B.M. (2001). Transcriptional regulation by p53 through intrinsic DNA/chromatin binding and site-directed cofactor recruitment. Mol. Cell *8*, 57–69.

Friedman, P.N., Chen, X., Bargonetti, J., and Prives, C. (1993). The p53 protein is an unusually shaped tetramer that binds directly to DNA. Proc. Natl. Acad. Sci. USA *90*, 3319–3323.

Funk, W.D., Pak, D.T., Karas, R.H., Wright, W.E., and Shay, J.W. (1992). A transcriptionally active DNA binding site for human p53 protein complexes. Mol. Cell. Biol. *12*, 2866–2871.

Gorina, S., and Pavletich, N.P. (1996). Structure of the p53 tumor suppressor bound to the ankyrin and SH3 domains of 53BP2. Science *274*, 1001–1005.

Haran, T.E., Joachimiak, A., and Sigler, P.B. (1992). The DNA target of the *trp* repressor. EMBO J. *11*, 3021–3030.

Inga, A., Storici, F., Darden, T.A., and Resnick, M.A. (2002). Differential transactivation by the p53 transcription factor is highly dependent on p53 level and promoter target sequence. Mol. Cell. Biol. *22*, 8612–8625.

Jayaraman, L., and Prives, C. (1999). Covalent and noncovalent modifiers of the p53 protein. Cell. Mol. Life Sci. *55*, 76–87.

Jeffrey, P.D., Gorina, S., and Pavletich, N.P. (1995). Crystal structure of the tetramerization domain of the p53 tumor suppressor at 1.7 angstroms. Science *267*, 1498–1502.

Joo, W.S., Jeffrey, P.D., Cantor, S.B., Finnin, M.S., Livingston, D.M., and Pavletich, N.P. (2002). Structure of the 53BP1 BRCT region bound to p53 and its comparison to the Brca1 BRCT structure. Genes Dev. *16*, 583–593.

Kaeser, M.D., and Iggo, R.D. (2002). Chromatin immunoprecipitation analysis fails to support the latency model for regulation of p53 DNA binding activity in vivo. Proc. Natl. Acad. Sci. USA *99*, 95–100.

Kim, E., and Deppert, W. (2006). The versatile interactions of p53 with DNA: when flexibility serves specificity. Cell Death Differ. *13*, 885–889.

Klein, C., Planker, E., Diercks, T., Kessler, H., Kunkele, K.P., Lang, K., Hansen, S., and Schwaiger, M. (2001). NMR spectroscopy reveals

the solution dimerization interface of p53 core domains bound to their consensus DNA. J. Biol. Chem. *276*, 49020–49027.

Ko, J., and Prives, C. (1996). p53: puzzle and paradigm. Genes Dev. *10*, 1054–1072.

Lavery, R., and Sklenar, H. (1989). Defining the structure of irregular nucleic acids: conventions and principles. J. Biomol. Struct. Dyn. *6*, 655–667.

Lee, W., Harvey, T.S., Yin, Y., Yau, P., Litchfield, D., and Arrowsmith, C.H. (1994). Solution structure of the tetrameric minimum transforming domain of p53. Nat. Struct. Biol. *1*, 877–890.

Levine, A.J. (1997). p53, the cellular gatekeeper for growth and division. Cell *88*, 323–331.

Liu, Y., Lagowski, J.P., Vanderbeek, G.E., and Kulesz-Martin, M.F. (2004). Facilitated search for specific genomic targets by p53 C-terminal basic DNA binding domain. Cancer Biol. Ther. *3*, 1102–1108.

Luscombe, N.M., Laskowski, R.A., and Thornton, J.M. (2001). Amino acid-base interactions: a three-dimensional analysis of protein-DNA interactions at an atomic level. Nucleic Acids Res. *29*, 2860–2874.

May, P., and May, E. (1999). Twenty years of p53 research: structural and functional aspects of the p53 protein. Oncogene *18*, 7621–7636.

McKinney, K., Mattia, M., Gottifredi, V., and Prives, C. (2004). p53 linear diffusion along DNA requires its C terminus. Mol. Cell *16*, 413–424.

McLure, K.G., and Lee, P.W.K. (1998). How p53 binds DNA as a tetramer. EMBO J. *17*, 3342–3350.

Mittl, P.R., Chene, P., and Grutter, M.G. (1998). Crystallization and structure solution of p53 (residues 326–356) by molecular replacement using an NMR model as template. Acta Crystallogr. D Biol. Crystallogr. *54*, 86–89.

Murshudov, G.N., Vagin, A.A., and Dodson, E.J. (1997). Refinement of macromolecular structures by the maximum-likelihood method. Acta Crystallogr. D Biol. Crystallogr. *53*, 240–255.

Nagaich, A., Zhurkin, V.B., Durrel, S.R., Jernigan, R.L., Appella, E., and Harrington, R.E. (1999). p53-induced DNA bending and twisting: p53 tetramer binds on the outer side of a DNA loop and increses DNA twisting. Proc. Natl. Acad. Sci. USA *96*, 1875–1880.

Olivier, M., Eeles, R., Hollstein, M., Khan, M.A., Harris, C.C., and Hainaut, P. (2002). The IARC TP53 database: new online mutation analysis and recommendations to users. Hum. Mutat. *19*, 607–614.

Oren, M. (2003). Decision making by p53: life, death and cancer. Cell Death Differ. *10*, 431–442.

Otwinowski, Z., and Minor, W. (1997). Processing of X-ray diffraction data collected in oscillation mode. In Methods in Enzymology, C.W. Carter, Jr., and M. Sweet, eds. (New York: Academic Press), pp. 307–326.

Prives, C., and Hall, P.A. (1999). The p53 pathway. J. Pathol. *187*, 112–126.

Qian, H., Wang, T., Naumovski, L., Lopez, C.D., and Brachmann, R.K. (2002). Groups of p53 target genes involved in specific p53 downstream effects cluster into different classes of DNA binding sites. Oncogene *21*, 7901–7911.

Resnick-Silverman, L., St Clair, S., Maurer, M., Zhao, K., and Manfredi, J.J. (1998). Identification of a novel class of genomic DNA-binding sites suggests a mechanism for selectivity in target gene activation by the tumor suppressor protein p53. Genes Dev. *12*, 2102–2107.

Rippin, T.M., Freund, S.M., Veprintsev, D.B., and Fersht, A.R. (2002). Recognition of DNA by p53 core domain and location of intermolecular contacts of cooperative binding. J. Mol. Biol. *319*, 351–358.

Rohaly, G., Chemnitz, J., Dehde, S., Nunez, A.M., Heukeshoven, J., Deppert, W., and Dornreiter, I. (2005). A novel human p53 isoform is an essential element of the ATR-intra-S phase checkpoint. Cell *122*, 21–32.

Samuels-Lev, Y., O'Connor, D.J., Bergamaschi, D., Trigiante, G., Hsieh, J.K., Zhong, S., Campargue, I., Naumovski, L., Crook, T., and Lu, X. (2001). ASPP proteins specifically stimulate the apoptotic function of p53. Mol. Cell *8*, 781–794.

Slickers, P., Hillebrand, M., Kittler, L., Lober, G., and Suhnel, J. (1998). Molecular modelling and footprinting studies of DNA minor groove binders: bisquaternary ammonium heterocyclic compounds. Anticancer Drug Des. *13*, 463–488.

Szak, S.T., Mays, D., and Pietenpol, J.A. (2001). Kinetics of p53 binding to promoter sites in vivo. Mol. Cell. Biol. *21*, 3375–3386.

Thornborrow, E.C., and Manfredi, J.J. (1999). One mechanism for cell type-specific regulation of the bax promoter by the tumor suppressor p53 is dictated by the p53 response element. J. Biol. Chem. *274*, 33747–33756.

Veprintsev, D.B., Freund, S.M., Andreeva, A., Rutledge, S.E., Tidow, H., Canadillas, J.M., Blair, C.M., and Fersht, A.R. (2006). Core domain interactions in full-length p53 in solution. Proc. Natl. Acad. Sci. USA *103*, 2115–2119.

Vogelstein, B., Lane, D., and Levine, A.J. (2000). Surfing the p53 network. Nature *408*, 307–310.

von Hippel, P.H., and Berg, O.G. (1989). Facilitated target location in biological systems. J. Biol. Chem. *264*, 675–678.

Vousden, K.H., and Lu, X. (2002). Live or let die: the cell's response to p53. Nat. Rev. Cancer *2*, 594–604.

Walker, D.R., Bond, J.P., Tarone, R.E., Harris, C.C., Makalowski, W., Boguski, M.S., and Greenblatt, M.S. (1999). Evolutionary conservation and somatic mutation hotspot maps of p53: correlation with p53 protein structural and functional features. Oncogene *18*, 211–218.

Wang, Y., Schwedes, J.F., Parks, D., Mann, K., and Tegtmeyer, P. (1995). Interaction of p53 with its consensus DNA-binding site. Mol. Cell. Biol. *15*, 2157–2165.

Waterman, J.L., Shenk, J.L., and Halazonetis, T.D. (1995). The dihedral symmetry of the p53 tetramerization domain mandates a conformational switch upon DNA binding. EMBO J. *14*, 512–519.

Wei, C.L., Wu, Q., Vega, V.B., Chiu, K.P., Ng, P., Zhang, T., Shahab, A., Yong, H.C., Fu, Y., Weng, Z., et al. (2006). A global map of p53 transcription-factor binding sites in the human genome. Cell *124*, 207–219.

Weinberg, R.L., Veprintsev, D.B., and Fersht, A.R. (2004). Cooperative binding of tetrameric p53 to DNA. J. Mol. Biol. *341*, 1145–1159.

Weinberg, R.L., Veprintsev, D.B., Bycroft, M., and Fersht, A.R. (2005). Comparative binding of p53 to its promoter and DNA recognition elements. J. Mol. Biol. *348*, 589–596.

Wolcke, J., Reimann, M., Klumpp, M., Gohler, T., Kim, E., and Deppert, W. (2003). Analysis of p53 "latency" and "activation" by fluorescence correlation spectroscopy. Evidence for different modes of high affinity DNA binding. J. Biol. Chem. *278*, 32587–32595.

Zhao, K., Chai, X., Johnston, K., Clements, A., and Marmorstein, R. (2001). Crystal structure of the mouse p53 core DNA-binding domain at 2.7 A resolution. J. Biol. Chem. *276*, 12120–12127.

Accession Numbers

Coordinates and structure factors for the four crystal structures (I, II, III, and IV) have been deposited in the RCSB Protein Data Bank with codes 2AC0, 2ATA, 2AHI, and 2ADY, respectively.